

# On Minimizing the Number of Running Buffers for Tabletop Rearrangement

Kai Gao Si Wei Feng Jingjin Yu

**Abstract**—For tabletop rearrangement problems with overhand grasps, storage space outside the tabletop workspace, or buffers, can temporarily hold objects which greatly facilitates the resolution of a given rearrangement task. This brings forth the natural question of how many running buffers are required so that certain classes of tabletop rearrangement problems are feasible. In this work, we examine the problem for both the labeled (where each object has a specific goal pose) and the unlabeled (where goal poses of objects are interchangeable) settings. On the structural side, we observe that finding the minimum number of running buffers (MRB) can be carried out on a dependency graph abstracted from a problem instance, and show that computing MRB on dependency graphs is NP-hard. We then prove that under both labeled and unlabeled settings, even for uniform cylindrical objects, the number of required running buffers may grow unbounded as the number of objects to be rearranged increases; we further show that the bound for the unlabeled case is tight. On the algorithmic side, we develop highly effective algorithms for finding MRB for both labeled and unlabeled tabletop rearrangement problems, scalable to over a hundred objects under very high object density. Employing these algorithms, empirical evaluations show that random labeled and unlabeled instances, which more closely mimics real-world setups, have much smaller MRBs.

## I. INTRODUCTION

In nearly all aspects of our everyday lives, be it work related, at home, or for play, objects are to be grasped and rearranged, e.g., tidying up a messy desk, cleaning the table after dinner, or solving a jigsaw puzzle. Similarly, many industrial and logistics applications require repetitive rearrangements of many objects, e.g., the sorting and packaging of products on conveyors with robots, and doing so efficiently is of critical importance to boost the competitiveness of the stakeholders. However, even without the challenge of grasping, deciding the sequence of objects for optimizing a rearrangement task is non-trivial. To that end, Han et al. [1] examined the problem of *tabletop object rearrangement with overhand grasps* (TORO), where objects may be picked up, moved around, and then placed at poses that are not in collision with other objects. An object that is picked up but cannot be directly placed at its goal is temporarily stored at a *buffer* location. For example, for the setup given in Fig. 1, using a single manipulator, either the Coke can or the Pepsi can must be moved to a buffer before the task can be completed. They show that computing a pick-n-place sequence that minimizes the use of the total number of

buffers is NP-hard and provide fast methods for computing that solution for problems with a couple dozen objects.



Fig. 1: A TORO instance where the three soda cans are to be rearranged from the left configuration to the right configuration.

In this study, we examine a more practical rearrangement objective which minimizes the number of *running buffers* (RB) needed for solving a TORO instance. We seek plans that minimize the maximum number of objects stored at buffers at any given moment. We denote this quantity as MRB (minimum running buffer). The objective is important because if the MRB required for solving a TORO instance exceeds the available buffer storage, which is always limited in practice, then the instance is infeasible. Therefore, the structural results and the algorithms that we present may be used not only for computing feasible and high-quality rearrangement plans, but they are also invaluable as a verification tool, e.g., to verify that a certain rearrangement setup will be able to solve most tasks for which it is designed to tackle.

The main technical contribution of this work is three-fold. First, we show that computing MRB on arbitrary *dependency graphs*, which encode the combinatorial information of TORO instances, is NP-hard. Second, we establish that for an  $n$ -object TORO instance, MRB can be lower bounded by  $\Omega(\sqrt{n})$  for uniform cylinders, even when all objects are *unlabeled*. This implies that the same is true for the *labeled* setting. Then, we provide a matching algorithmic upper bound  $O(\sqrt{n})$  for the unlabeled setting. Last but not least, we develop multiple highly effective and optimal algorithms for computing rearrangement plans with MRB for TORO. In particular, we present a dynamic programming method for the labeled setting, a priority queue-based algorithm for the unlabeled setting, and a much more efficient *depth-first-search dynamic programming* routine that readily scales to instances with over a hundred objects for both settings. Furthermore, we provide methods for computing plans with the minimum number of *total buffers* subject to the MRB constraints.

**Related work.** As a high utility capability, manipulation of objects in a bounded workspace has been extensively studied, with works devoted to perception/scene understanding [2]–[5], task/rearrangement planning [1], [6]–[15], manipulation [16]–[23], as well as integrated holistic approaches [24]–[28]. As object rearrangement problems often embed within

The authors are with the Department of Computer Science, Rutgers, the State University of New Jersey, Piscataway, NJ, USA. E-Mails: {kai.gao, siwei.feng, jingjin.yu}@rutgers.edu. This work is supported in part by NSF awards IIS-1734419, IIS-1845888, and CCF-1934924.

them multi-robot motion planning problems, rearrangement inherits the PSPACE-hard complexity [29]. These problems remain NP-hard even without complex geometric constraints [30]. Considering rearrangement plan quality, e.g., minimizing the number of pick-n-places or the end-effector travel, is also computationally intractable [1].

For rearrangement tasks using mainly prehensile actions, the algorithmic studies of Navigation Among Movable Obstacles [7], [31] result in backtracking search methods that can effectively deal with monotone and other instances with “nice” properties. Via carefully calling monotone solvers, difficult non-monotone cases can be solved as well [11]. Han et al. [1] relates tabletop rearrangement problems to the Traveling Salesperson Problem [32] and the Feedback Vertex Set problem [33], both of which are NP-hard. Nevertheless, integer linear programming models are shown to quickly compute high quality solutions for practical sized (e.g., 1-2 dozen of objects) problems. Focusing mainly on the unlabeled setting, bounds on the number of pick-n-places are provided under different assumptions on disk objects in [34]. In [14], a complete algorithm is developed that reasons about object retrieval, rearranging other objects as needed, with later work [35] considering plan optimality and sensor occlusion. While the objectives in most problems focus on the number of motions, Halperin et al. [36] examined space-aware reconfiguration in which disc objects move along straight lines in the workspace, seeking to minimize space needed to carry out a rearrangement task.

Non-prehensile rearrangement has also been extensively studied, with singulation as an early focus [37]–[39]. Iterative search was employed in [13] for accomplishing a multitude of rearrangement tasks spanning singulating, separation, and sorting of identically shaped cubes. Song et al. [40] combines Monte Carlo Tree Search with a deep policy network for separating many objects into coherent clusters within a bounded workspace, supporting non-convex objects. More recently, a bi-level planner is proposed [15], engaging both (non-prehensile) pushing and (prehensile) overhand grasping for sorting a large number of objects.

On the structural side, a central object that we study is the *dependency graph* [41] structure. We observe that, in the labeled setting, through the dependency graph, the running buffer problems naturally connect to *graph layout* problems [42]–[47], where an optimal linear ordering of graph vertices is sought. Graph layout problems find a vast number of important applications including VLSI design, scheduling [48], and so on. For the unlabeled setting, the dependency graph becomes a planar one for uniform objects with a square or round base. Rearrangement can be tackled through partitioning of the dependency graph using a *vertex separator* [49]–[52]. For a survey on these topics, see [42].

**Paper organization.** The rest of the paper is organized as follows. We introduce the MRB focused rearrangement problems and discuss the associated dependency graphs in Sec. II. Then, in Sec. III, we establish some basic structural properties of the optimality structure of the problems, and show that minimizing running buffer size on dependency

graphs is computationally intractable. We proceed to establish the lower and upper bounds on MRB in Sec. IV and describe our proposed algorithmic solutions in Sec. V. Evaluation follows in Sec. VI. We conclude with Sec. VII.

## II. PRELIMINARIES

We describe two practical (labeled and unlabeled) formulations of the tabletop object rearrangement problems using external buffers, and discuss the important *dependency graph* structure for both settings.

### A. Labeled Tabletop Rearrangement with External Buffers

Consider a bounded workspace  $\mathcal{W} \subset \mathbb{R}^2$  with a set of  $n$  objects  $\mathcal{O} = \{o_1, \dots, o_n\}$  placed inside it. All objects are assumed to be *generalized cylinders* with the same height. A *feasible arrangement* of these objects is a set of poses  $\mathcal{A} = \{x_1, \dots, x_n\}, x_i \in SE(2)$  in which no two objects collide. Let  $\mathcal{A}_1 = \{x_1^s, \dots, x_n^s\}$  and  $\mathcal{A}_2 = \{x_1^g, \dots, x_n^g\}$  be two feasible arrangements, a tabletop object rearrangement problem [1] seeks a plan using *pick-n-place* operations that move the objects from  $\mathcal{A}_1$  to  $\mathcal{A}_2$  (see Fig. 2(a) for an example with 7 uniform cylinders). In each pick-n-place operation, an object is grasped by a robot arm, lifted above all other objects, transferred to and lowered at a new pose  $p \in SE(2)$  where the object will not be in collision with other objects, and then released. A pick-n-place operation can be formally represented as a 3-tuple  $a = (i, x', x'')$ , denoting that object  $o_i$  is moved from pose  $x'$  to pose  $x''$ . A full rearrangement plan  $P = (a_1, a_2, \dots)$  is then an ordered sequence of pick-n-place operations.

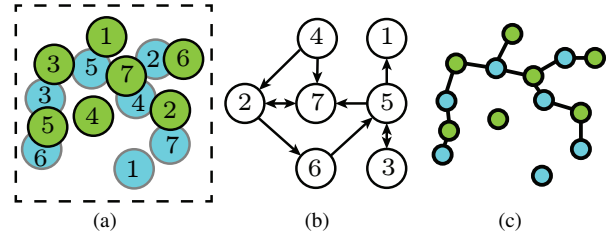


Fig. 2: A 7-object labeled instance with uniform cylinders; we will use this instance as a running example. (a) The green discs (as projections of cylinders) represent the start arrangement  $\mathcal{A}_1$  and the cyan discs represent the goal arrangement  $\mathcal{A}_2$ . (b) The corresponding labeled dependency graph. (c) The corresponding unlabeled dependency graph, which is bipartite and planar.

Depending on  $\mathcal{A}_1$  and  $\mathcal{A}_2$ , it may not always be possible to directly transfer an object  $o_i$  from  $x_i^s$  to  $x_i^g$  in a single pick-n-place operation, because  $x_i^g$  may be occupied by other objects. This creates *dependencies* between objects. If object  $o_i$  at pose  $x_i^g$  intersects object  $o_j$  at pose  $x_j^s$ , we say  $o_i$  *depends* on  $o_j$ . This suggests that object  $o_j$  must be moved first before  $o_i$  can be placed at its goal pose  $x_i^g$ .

It is possible to have circular dependencies, e.g., between objects 3 and 5 in Fig. 2(a). In such cases, some object(s) must be temporarily moved to an intermediate pose to solve the rearrangement problem. Similar to [1], we assume that *external buffers* outside of the workspace are used for assuming intermediate poses, which avoids time-consuming geometric computations if the intermediate poses are to be placed within  $\mathcal{W}$ . During the execution of a rearrangement

plan, there can be multiple objects that are stored at buffer locations. We call the buffers currently being used as *running buffers* (RB). With the introduction of buffers, there are three types of pick-n-place operations: 1) pick an object at its start pose and place at a buffer, 2) pick an object at its start pose and place at its goal pose, and 3) pick an object from buffer and place at its goal pose. Notice that buffer poses are not important. Naturally, it is desirable to be able to solve a rearrangement problem with the least number of running buffers, yielding the running buffer minimization problem.

**Problem 1** (Labeled Running Buffer Minimization (LRBM)). *Given feasible arrangements  $\mathcal{A}_1$  and  $\mathcal{A}_2$ , find a rearrangement plan  $P$  that minimizes the maximum number of running buffers used at any given time.*

In an LRBM instance, the set of all dependencies induced by  $\mathcal{A}_1$  and  $\mathcal{A}_2$  can be represented using a directed graph  $G_{\mathcal{A}_1, \mathcal{A}_2}^\ell = (V, A)$ , where each  $v_i \in V$  corresponds to object  $o_i$  and there is an arc  $v_i \rightarrow v_j$  for  $1 \leq i, j \leq n, i \neq j$  if object  $o_i$  depends on object  $o_j$ . We call  $G_{\mathcal{A}_1, \mathcal{A}_2}^\ell$  a *labeled dependency graph*. The labeled dependency graph for Fig. 2(a) is given in Fig. 2(b). We can immediately identify multiple circular dependencies in the graph, e.g., between objects 3 and 5, or among objects 7, 2, 6 and 5. It is not difficult to see that the dependency graph abstraction fully captures the information needed to solve a tabletop rearrangement problem with external buffers.

#### B. Unlabeled Tabletop Rearrangement Problem

In an unlabeled setting, objects are interchangeable. That is, it does not matter which object goes to which goal. For example, in Fig. 2, object 5 can move to the goal for object 6. We call this version the Unlabeled Running Buffer Minimization (URBM) problem, which is intuitively easier. The plan for the unlabeled problem can be represented similarly as the labeled setting; we continue to use labels but do not require matching labels for start and goal poses.

For the unlabeled setting, there clearly remains dependency between start and goal arrangements, but in a different form. We update the *unlabeled* dependency graph for URBM as an undirected *bipartite* graph between the start arrangement and the goal arrangement. That is,  $G_{\mathcal{A}_1, \mathcal{A}_2}^u = (V_1 \cup V_2, E)$  where each  $v \in V_1$  (resp.,  $v \in V_2$ ) corresponds to a start (resp., goal) pose  $p \in \mathcal{A}_1$  (resp.,  $p \in \mathcal{A}_2$ ). We denote the vertices representing the start and goal poses as *start vertices* and *goal vertices*, respectively. There is an edge between  $v_1 \in V_1$  and  $v_2 \in V_2$  if the objects at the corresponding poses overlap. The unlabeled dependency graph for Fig. 2(a) is given in Fig. 2(c).

We make a straightforward but important observation of the unlabeled dependency graph when objects are uniform cylinders, which is a key sub-class of TORO problems, e.g., many products can be approximated as uniform cylinders.

**Proposition II.1.** *For unlabeled tabletop object rearrangement problems where all objects are identical cylinders, the unlabeled dependency graph is a planar bipartite graph with maximum degree 5.*

*Proof.* The bipartite and planar part come directly from the problem setup. Since we work with uniform cylinders which have uniform disc base, one disc may only touch six non-overlapping discs and non-trivially intersect at most five non-overlapping discs.  $\square$

### III. STRUCTURAL ANALYSIS AND NP-HARDNESS

In this section, we highlight some important structural properties of LRBM, including (1) the comparison to minimizing the total number of buffers [1], (2) the solutions of LRBM and the *linear arrangement* [53] or *linear ordering* [54] of its dependency graph, and (3) the hardness of computing MRB for labeled dependency graphs.

#### A. Running Buffer versus Total Buffer

As mentioned in the introduction, running buffers are related to but different from the total number of buffers required, as studied in [1], to solve a rearrangement problem using external buffers. It was shown that the minimum number of total buffers for solving an LRBM is the same as the size of the minimum *feedback vertex set* (FVS) of the underlying dependency graph. An FVS is a set of vertices the removal of which leaves a graph acyclic. An LRBM with an acyclic dependency graph can be solved without using any buffer. We denote the size of the minimum FVS as MFVS.

As an example, for LRBM, consider a labeled dependency graph that is formed by  $n$  copies of 2-cycles. The MFVS is  $n$ . On the other hand, the MRB is just 1 for the problem. That is, only a single external buffer is needed to solve the problem. Therefore, whereas the total number of buffers used has more bearing on global solution optimality, MRB sheds more light on *feasibility*. Knowing the MRB tells us whether a certain number of external buffers will be sufficient for solving a class of rearrangement problems. This is critical for practical applications where the number of external buffers is generally limited to be a small constant.

We give an example where the MRB and MFVS cannot always be optimized simultaneously. For the setup (Fig. 3) where objects have convex footprints, the MFVS,  $\{7, 9, 10\}$ , has size 3. Using our algorithms, to be detailed later, the MRB is 2 (e.g., with the sequence 10, 8, 4, 5, 3, 6, 7, 1, 2, 9, the interpretation of which is given in Sec. III-B). However, constrained on MRB = 2, the total number of buffers that must be used is at least  $4 > 3$ . We note that, this is rarely the case; for uniform cylinders, the total number of buffers needed after first minimizing the running buffer is almost always the same as the MFVS size.

#### B. Linear Ordering of Graph Vertices and Running Buffer

Given a graph with vertex set  $V$ , a *linear ordering* of  $V$  is a bijective function  $\varphi : \{1, \dots, |V|\} \rightarrow V$ . Given a dependency graph  $G = (V, A)$  for an LRBM and a linear ordering  $\varphi$ , we may turn it into a plan  $P$  by sequentially picking up objects corresponding to vertices  $\varphi(1), \varphi(2), \dots$ . For each object that is picked up, it is moved to its goal pose if it has no further dependencies; otherwise, it is stored in the buffer. Objects already in the buffer will be moved to their goal pose at the earliest possible opportunity.

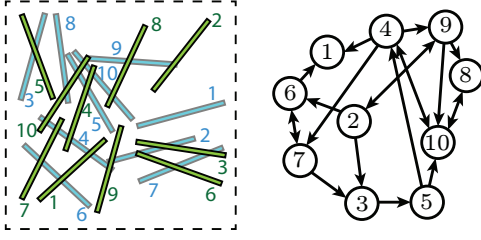


Fig. 3: An LRBM instance with uniform thin cuboids (left) and its labeled dependency graph, where the total number of buffers needed is more than the size of the MFVS when the number of running buffers is minimized.

For example, given the linear ordering 1, 5, 6, 3, 4, 2, 7 for the dependency graph from Fig. 2(b), first,  $o_1$  can be directly moved to its goal. Then,  $o_5$  is moved to the buffer because it has dependency on  $o_3$  and  $o_7$  (but no longer on  $o_1$ ). Then,  $o_6$  can be directly moved to the buffer because  $o_5$  is now at a buffer location. Similarly,  $o_3$  can be moved to its goal next. Then,  $o_4$  and  $o_2$  must be moved to buffer, after which  $o_7$  can be moved to its goal directly. Finally,  $o_2$ ,  $o_4$ , and  $o_5$  can be moved to their respective goals from the buffer. This leads to a maximum running buffer size of 3. This is not optimal; an optimal sequence is 5, 6, 2, 7, 4, 3, 1, with MRB = 2. Both sequences are illustrated in Fig. 4.

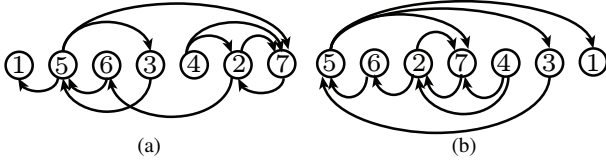


Fig. 4: Two linear orderings of vertices of the labeled dependency graph from Fig. 2(b). The right one minimizes MRB.

From the discussion, we may view the number of running buffers as a function of a dependency graph  $G$  and a linear ordering  $\varphi$ , i.e.,  $\text{RB}(G, \varphi)$  is the number of running buffers needed for rearranging  $G$  following the order given by  $\varphi$ . We then have  $\text{MRB}(G) = \min_{\varphi} \text{RB}(G, \varphi)$ .

### C. Intractability of Computing $\text{MRB}(G)$

Since computing MFVS is NP-hard [1], one would expect that computing MRB for a labeled dependency graph, which can be any directed graph, is also hard. We show that this is indeed the case, through examining the interesting relationship between MRB and the *vertex separation problem* (VSP), which is equivalent to path width, gate matrix layout and search number problems as described in Theorem 3.1 in [42], resulting from a series of studies [55]–[57]. Unless  $P = NP$ , there cannot be an absolute approximation algorithm for any of these problems [47]. First, we describe the vertex separation problem. Intuitively, given an undirected graph  $G = (V, E)$ , VSP seeks a linear ordering  $\varphi$  of  $V$  such that, for a vertex with order  $i$ , the number of vertices come no later than  $i$  in the ordering, with edges to vertices that come after  $i$ , is minimized.

### Vertex Separation (VSP)

**Instance:** Graph  $G(V, E)$  and an integer  $K$ .

**Question:** Is there a bijective function  $\varphi : \{1, \dots, n\} \rightarrow V$ , such that for any integer  $1 \leq i \leq n$ ,  $|\{u \in V \mid \exists (u, v) \in E \text{ and } \varphi(u) \leq i < \varphi(v)\}| \leq K$ ?

As an example, in Fig. 5(a), with the given linear ordering, at the second vertex, both the first and the second vertices have edges crossing the vertical separator, yielding a crossing number of 2. Given a graph  $G$  and a linear ordering  $\varphi$ , we define  $\text{VS}(G, \varphi) := \max_i |\{u \in V \mid \exists (u, v) \in E \text{ and } \varphi(u) \leq i < \varphi(v)\}|$ . VSP seeks  $\varphi$  that minimizes  $\text{VS}(G, \varphi)$ . Let  $\text{MINVS}(G)$ , the vertex separation number of graph  $G$ , be the minimum  $K$  for which a VSP instance has a yes answer, then  $\text{MINVS}(G) = \min_{\varphi} \text{VS}(G, \varphi)$ . Now, given an undirected graph  $G$  and a labeled dependency graph  $G^\ell$  obtained from  $G$  by replacing each edge of  $G$  with two directed edges in opposite directions, we observe that there are clear similarities between  $\text{VS}(G, \varphi)$  and  $\text{RB}(G^\ell, \varphi)$ , which is characterized in the following lemma.

**Lemma III.1.**  $\text{VS}(G, \varphi) \leq \text{RB}(G^\ell, \varphi) \leq \text{VS}(G, \varphi) + 1$ .

*Proof sketch.* Fixing a linear ordering  $\varphi$ , it is clear that  $\text{VS}(G, \varphi) \leq \text{RB}(G^\ell, \varphi)$ , since the vertices on the left side of a separator with edges crossing the separator for  $G$  corresponds to the objects that must be stored at buffer locations. For example, in Fig. 5(a), past the second vertex from the left, both the first and the second vertices have edges crossing the vertical “separator”. In the corresponding dependency graph shown in Fig. 5(b), objects corresponding to both vertices must be moved to the external buffer. On the other hand, we have  $\text{RB}(G^\ell, \varphi) \leq \text{VS}(G, \varphi) + 1$  because as we move across a vertex in the linear ordering, the corresponding object may need to be moved to a buffer location temporarily. For example, as the third vertex from the left in Fig. 5(a) is passed, the vertex separator drops from 2 to 1, but for dealing with the corresponding dependency graph in Fig. 5(b), the object corresponding to the third vertex from the left must be moved to the buffer before the first and the second objects stored in buffer can be placed at their goals.  $\square$

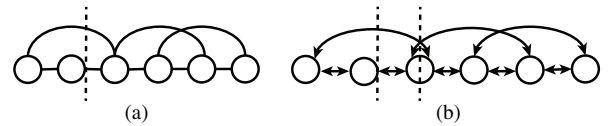


Fig. 5: (a) An undirected graph and a linear ordering of its vertices. (b) A corresponding labeled dependency graph with the same vertex ordering.

**Theorem III.1.** *Computing MRB, even with an absolute approximation, for a labeled dependency graph is NP-hard.*

*Proof.* Given an undirected graph  $G$ , we reduce from approximating VSP within a constant to approximating MRB within a constant for a dependency graph  $G^\ell$  from  $G$  constructed as stated before, replacing each edge in  $G$  as a bidirectional dependency.



Unless  $P = NP$ , VSP does not have absolute approximation in polynomial time. Henceforth, if  $\text{MRB}(G^\ell, \varphi)$  can be approximated within  $\alpha$  in polynomial time, which means for graph  $G$ , we can find a  $\varphi^*$  in polynomial time such that  $\text{RB}(G^\ell, \varphi^*) \leq \text{MRB}(G^\ell) + \alpha$ , we then have  $\text{VS}(G, \varphi^*) \leq \text{RB}(G^\ell, \varphi^*) \leq \alpha + \text{MRB}(G^\ell) \leq \text{MINVS}(G) + \alpha + 1$ , which shows vertex separation can have an absolute approximation, implying  $P = NP$ .  $\square$

#### IV. LOWER AND UPPER BOUNDS ON MRB

We proceed to establish bounds on MRB, i.e., what is the lowest possible MRB for LRBM and URBM, and what is the best that we can do to lower MRB? An important outcome is that MRB can grow unbounded with the number of objects, even for URBM when objects are all uniform cylinders. Another very interesting result is that we are able to close the gap between lower and upper bound for URBM for uniform cylinders.

##### A. Intrinsic MRB Lower Bounds

When there is no restrictions on object footprint, MRB can easily reach the maximum possible  $n - 1$  for an  $n$  object instance, even in the URBM case. Such an example is given in Fig. 6, where  $n = 6$  thin cuboids are aligned horizontally in  $\mathcal{A}_1$ , one above the other. The cuboids are vertically aligned in  $\mathcal{A}_2$ , and every pair of start pose and goal pose induces a collision. Clearly, this yields a bidirectional  $K_6$  labeled dependency graph in the LRBM case and a  $K_{6,6}$  unlabeled dependency graph in the URBM case. For both,  $n - 1 = 5$  objects must be moved to buffer before the problem can be resolved. The example clearly can be generalized to an arbitrary number of objects.

**Proposition IV.1.** *MRB lower bound is  $n - 1$  for  $n$  objects for both LRBM and URBM, which is the maximum possible, even for uniform convex shaped objects.*

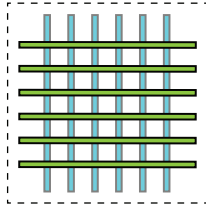


Fig. 6: An instance with 6 cuboids where horizontal and vertical sets represent start and goal poses, respectively.

The lower bound on MRB being  $\Omega(n)$  is undesirable, but it is established using objects that are “thin”. Everyday objects are not often like that. An ensuing question of high practical value is then: what happens when the footprint of the objects are “nicer”? Next, we show that, the lower bound drops to  $\Omega(\sqrt{n})$  for uniform cylinders, which approximate many real-world objects/products. Further more, we show that this lower bound is tight for URBM (in Section IV-B).

We first establish the  $\Omega(\sqrt{n})$  lower bound for URBM. For convenience, assume  $n$  is a perfect square, i.e.,  $n = m^2$  for some integer  $m$ . To get to the proof, a grid-like unlabeled dependency graph is used, which we call a *dependency grid*, where  $\mathcal{A}_1$  and  $\mathcal{A}_2$  have fixed grid (rotated by  $\pi/4$ ) patterns,

an example of which is given in Fig. 7. We use  $\mathcal{D}(w, h)$  to denote a dependency grid with  $w$  columns and  $h$  rows. Let  $(x, y)$  be the coordinate of a vertex  $v_{x,y}$  on  $\mathcal{D}(w, h)$  with the top left being  $(1, 1)$ . The parity of  $x + y$  determines the partite set of the vertex (recall that unlabeled dependency graph for uniform cylinders is always a planar bipartite graph, by Proposition II.1), which may correspond to a start pose or a goal pose. With this in mind, we simply call vertices of  $\mathcal{D}(w, h)$  start and goal vertices; let  $v_{1,1}$  be a start vertex.

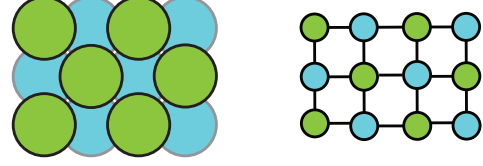


Fig. 7: A URBM instance (left) and its unlabeled dependency graph (right), a  $4 \times 3$  dependency grid. Green and cyan indicate start and goal arrangements, respectively.

We use  $\mathcal{D}(m, 2m)$  for establishing the lower bound on MRB. We use a *vertex pair*  $p_{i,j}$  to refer to two adjacent vertices  $v_{i,2j-1}$  and  $v_{i,2j}$  in  $\mathcal{D}(m, 2m)$ . It is clear that a vertex pair contains a start and a goal vertex. We say that a goal vertex is *filled* if an object is placed at the corresponding goal pose. We say that a start vertex (which belongs to a vertex pair) is *cleared* if the corresponding object at the vertex is picked (either put at a goal or at a buffer) but the corresponding goal in the vertex pair is not filled. At any moment when the robot is not holding an object, the number of objects in the buffer is the same as the number of cleared vertices. For each column  $i$ ,  $1 \leq i \leq m$ , let  $f_i$  (resp.,  $c_i$ ) be the number of goal (resp., start) vertices in the column that are filled (resp., cleared). Notice that a goal cannot be filled until the object at the corresponding start vertex is removed.

**Lemma IV.1.** *On a dependency grid  $\mathcal{D}(m, 2m)$ , for two adjacent columns  $i$  and  $i + 1$ ,  $1 \leq i < m$ , if  $f_i + f_{i+1} \neq 0$  or  $2m$ , then  $c_i + c_{i+1} \geq 1$ . In other words, there is at least one cleared vertex in the two adjacent columns unless  $f_i = f_{i+1} = 0$  or  $f_i = f_{i+1} = m$ .*

*Proof.* If there is a  $j$ ,  $1 \leq j \leq m$ , such that only one of the goal vertices in vertex pairs  $p_{i,j}$  and  $p_{i+1,j}$  is filled (Fig. 8(a)), then the start vertex in the other vertex pair must be cleared. Therefore,  $c_i + c_{i+1} \geq 1$ .

On the other hand, if, for each  $j$ ,  $1 \leq j \leq m$ , both or neither of the goal vertices in  $p_{i,j}$  and  $p_{i+1,j}$  is filled, then there is a  $j$ ,  $1 \leq j \leq m - 1$ , such that both goal vertices in  $p_{i,j}$  and  $p_{i+1,j}$  are filled but neither of those in  $p_{i,j+1}$  and  $p_{i+1,j+1}$  is filled (Fig. 8(b)) or the opposite (Fig. 8(c)). Then, for the vertex pairs whose goal vertices are not filled, say  $p_{i,j+1}$  and  $p_{i+1,j+1}$ , one of their start vertices is a neighbor of the filled goal in  $p_{i,j}$  and  $p_{i,j+1}$ . Therefore, at least one of the start vertices in  $p_{i,j+1}$  and  $p_{i+1,j+1}$  is a cleared vertex. And thus,  $c_i + c_{i+1} \geq 1$ .  $\square$

**Lemma IV.2.** *Given a URBM instance with  $n = m^2$  objects and whose dependency graph is  $\mathcal{D}(m, 2m)$ , its MRB is lower bounded by  $\Omega(m) = \Omega(\sqrt{n})$*

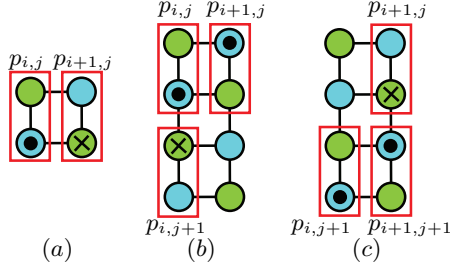


Fig. 8: Some cases discussed in the lemma IV.1. The green and cyan nodes represent the start and goal vertices in the dependency graph. Specifically, the cyan nodes with a dot inside represent the filled vertices and the green nodes with a cross inside represent the cleared vertices. (a) When only one goal vertex in  $p_{i,j}$  and  $p_{i+1,j}$  is filled up, the start vertex in the other vertex pair is a cleared vertex. (b) When both goal vertices in  $p_{i,j}$  and  $p_{i+1,j}$  are filled but neither of those in  $p_{i,j+1}$  and  $p_{i+1,j+1}$  is filled, one of the start vertices  $p_{i,j+1}$  and  $p_{i+1,j+1}$  is a cleared vertex. (c) The opposite case of (b).

*Proof.* We show that there are  $\Omega(m)$  cleared vertices when  $\lfloor n/3 \rfloor$  goal vertices are filled. Suppose there are  $q$  columns in  $\mathcal{D}$  with  $1 \leq f_i \leq m-1$ . According to the definition of  $f_i$ , for each of these  $q$  columns, there is at least one goal vertex that is filled and at least one goal vertex that is not.

If  $q < \frac{\lfloor n/3 \rfloor}{3(m-1)}$ , then there are two columns  $i$  and  $j$ , such that  $f_i = m$  and  $f_j = 0$ . That is because  $\sum_{1 \leq i \leq m} f_i = \lfloor n/3 \rfloor$  and  $0 \leq f_i \leq m$  for all  $1 \leq i \leq m$ . Therefore, for the vertex pairs in each row  $j$ , at least one goal vertex is filled but at least one is not. And thus, for each  $j$ , there are two adjacent columns  $i, i+1$ ,  $1 \leq i < m$ , such that there is only one goal vertex in  $p_{i,j}$  and  $p_{i+1,j}$  is filled and the start vertex in the other vertex pair is cleared (Fig. 8(a)). Therefore, there are at least  $m$  cleared vertices in this case.

If  $q \geq \frac{\lfloor n/3 \rfloor}{3(m-1)}$ , then we partition all the columns in  $\mathcal{D}$  into  $\lfloor m/2 \rfloor$  disjoint pairs: (1,2), (3,4), ... The  $q$  columns belong to at least  $\lfloor q/2 \rfloor$  pairs of adjacent columns. Therefore, according to Lemma IV.1, we have  $\Theta(m)$  cleared vertices.

In conclusion, there are  $\Omega(m)$  cleared vertices when there are  $\lfloor n/3 \rfloor$  filled goal. Therefore, the minimum MRB of this instance is  $\Omega(m)$ .  $\square$

Because a URBM always have lower MRB than an LRBM with the same objects and goal placements, the conclusion of Lemma IV.2 directly applies to LRBM. Therefore, we have

**Theorem IV.1.** *For both URBM and LRBM with  $n$  uniform cylinders, MRB is lower bounded by  $\Omega(\sqrt{n})$ .*

For uniform cylinders, while the lower bound on URBM is tight (as shown in Section IV-B), we do not know whether the lower bound on LRBM is tight; our conjecture is that  $\Omega(\sqrt{n})$  is not a tight lower bound for LRBM. Indeed, the  $\Omega(\sqrt{n})$  lower bound can be realized when uniform cylinders are simply arranged on a cycle, an illustration of which is given in Fig. 9. For a general construction, for each object  $o_i$ , let  $o_i$  depend on  $o_{(i-1) \bmod n}$  and  $o_{(i+\sqrt{n}) \bmod n}$ , where  $n$  is the number of objects in the instance. From the labeled dependency graph, we can construct the actual

LRBM instance where start and goal arrangements both form a cycle. We can show that when  $n/2$  objects are at the goal poses,  $\Omega(\sqrt{n})$  objects are at the buffer. We omit the proof, which is similar in spirit to that for Lemma IV.2.

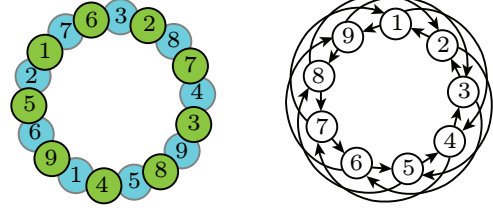


Fig. 9: An example of a 9-object LRBM yielding  $\Omega(\sqrt{n})$  MRB (left) and the corresponding dependency graph (right).

## B. MRB Algorithmic Upper Bounds

We now establish that regardless of how  $n$  uniform cylinders are to be rearranged, the corresponding URBM instance admits a solution using  $O(\sqrt{n})$  running buffers. The lower and upper bounds on URBM agree; therefore, the  $O(\sqrt{n})$  bound is tight.

To prove the upper bound, We propose an  $O(n \log(n))$ -time algorithm SEPPLAN for the setting based on a vertex separator of  $G_{\mathcal{A}_1, \mathcal{A}_2}^u$ . SEPPLAN computes a sequence of goal vertices to be removed from the dependency graph. Given a sequence of goal vertices to be removed, the running buffer size at each moment equals

$$\max(0, \|N(g, G_{\mathcal{A}_1, \mathcal{A}_2}^u)\| - \|g\|)$$

where  $g$  is the set of removed goal vertices at this moment, and  $N(g, G_{\mathcal{A}_1, \mathcal{A}_2}^u)$  is the set of neighbors of  $g$  in  $G_{\mathcal{A}_1, \mathcal{A}_2}^u$ . We prove that SEPPLAN can find a rearrangement plan with  $O(\sqrt{n})$  running buffers.

### Algorithm 1: SEPPLAN

---

**Input :**  $G_{\mathcal{A}_1, \mathcal{A}_2}^u(V, E)$ : unlabeled dependency graph  
**Output:**  $\pi$ : goal sequence

- 1  $\pi, V, E \leftarrow \text{RemovalTrivialGoals}(G_{\mathcal{A}_1, \mathcal{A}_2}^u(V, E))$
- 2 **if**  $V$  is  $\emptyset$  **then return**  $\pi$  ;
- 3  $A, B, C \leftarrow \text{Separator}(G_{\mathcal{A}_1, \mathcal{A}_2}^u(V, E))$
- 4  $\pi \leftarrow \pi + g(C)$
- 5  $A' \leftarrow A - N(g(C), G_{\mathcal{A}_1, \mathcal{A}_2}^u(V, E))$
- 6  $B' \leftarrow A - N(g(C), G_{\mathcal{A}_1, \mathcal{A}_2}^u(V, E))$
- 7  $\pi_{A'} \leftarrow \text{SEPPLAN}(G_{\mathcal{A}_1, \mathcal{A}_2}^u(A', E(A')))$
- 8  $\pi_{B'} \leftarrow \text{SEPPLAN}(G_{\mathcal{A}_1, \mathcal{A}_2}^u(B', E(B')))$
- 9 **if**  $|g(A')| - |s(A')| \geq |g(B')| - |s(B')|$  **then**  
 $\pi \leftarrow \pi + \pi_{A'} + \pi_{B'}$  ;
- 10 **else**  $\pi \leftarrow \pi + \pi_{B'} + \pi_{A'}$  ;
- 11 **return**  $\pi$

---

The algorithm is presented in Algo. 1. SEPPLAN consumes a graph  $G_{\mathcal{A}_1, \mathcal{A}_2}^u(V, E)$ , which is a subgraph of  $G_{\mathcal{A}_1, \mathcal{A}_2}^u$  induced by vertex set  $V$ . To start with, the isolated goal vertices or those with only one dependency in  $G_{\mathcal{A}_1, \mathcal{A}_2}^u(V, E)$  can be removed without using buffers (Line 1). After that,  $V$  can be partitioned into three disjoint subsets  $A$ ,  $B$  and  $C$  [49] (Line 3), such that there is no edge connecting vertices in  $A$  and  $B$ ,  $|A|, |B| \leq 2|V|/3$ , and  $|C| \leq 2\sqrt{2|V|}$  (Fig. 10(a)). For the start vertices in  $C$  and the neighbors of the goal vertices in  $C$ , we remove them from  $G_{\mathcal{A}_1, \mathcal{A}_2}^u$ . Since there are at most 5 neighbors for each goal vertex, there are at most  $10\sqrt{2|V|}$  objects moved to the buffer in this operation.

After that, we remove the goal vertices in  $C$ , which should be isolated now (Line 4). Function  $g(\cdot)$  obtains the goal vertices in a given vertex set. Let  $A'$ ,  $B'$  be the remaining vertices in  $A$  and  $B$  (Line 5-6). Function  $N(\cdot, \cdot)$  obtains the neighbors of a vertex set in a given dependency subgraph. With the removal of  $C$  from  $G_{A_1, A_2}^u$ ,  $A'$  and  $B'$  form two independent subgraphs (Fig. 10(b)). We can deal with the subgraphs one after the other by recursively calling SEPPLAN (Fig. 10(c)) (Line 7-8). Let  $\delta(V') := |g(V')| - |s(V')|$  where  $g(V')$  and  $s(V')$  are the goal and start vertices in a vertex set  $V'$  respectively. Between vertex subsets  $A'$  and  $B'$ , we prioritize the one with larger  $\delta(\cdot)$  value (Line 9-10).

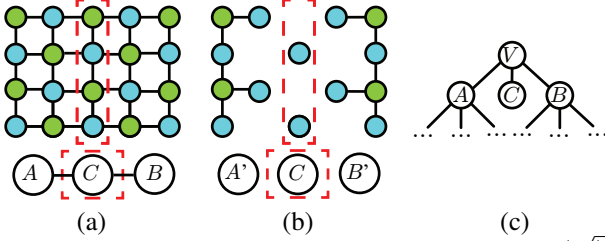


Fig. 10: The recursive solver SEPPLAN for URBM. (a) A  $O(\sqrt{|V|})$  vertex separator for the planar dependency graph. (b) By removing the start vertices in  $C$  and the neighbors of the goal vertices in  $C$ , the remaining graph consists of two independent subgraphs and isolated goal poses in  $C$ . (c) The problem can be solved by recursively calling SEPPLAN.

To investigate the running buffer size of the plan computed by SEPPLAN, we construct a binary tree  $T$  based on SEPPLAN (Fig. 10(c)). Each node represents a recursive call consuming a subgraph  $G_{A_1, A_2}^u(V, E)$  and the left and right children of the node are induced from subgraphs  $G_{A_1, A_2}^u(A', E(A'))$  and  $G_{A_1, A_2}^u(B', E(B'))$  of  $G_{A_1, A_2}^u(V, E)$ . SEPPLAN computes the plan by visiting the binary tree in a depth-first manner. For each node on  $T$ , given the input dependency graph  $G_{A_1, A_2}^u(V, E)$ , denote the sequence before we deal with  $G_{A_1, A_2}^u(V, E)$  as  $\pi_0$ . Denote the vertices pruned in RemovalTrivialGoals( $G_{A_1, A_2}^u(V, E)$ ) as  $P$ . Without loss of generality, assume that SEPPLAN recurses into  $A'$  before  $B'$ . Let  $\pi_P$ ,  $\pi_{C'}$ ,  $\pi_{A'}$  and  $\pi_{B'}$  be the goal removal sequence after we remove vertices in  $P$ ,  $C'$ ,  $A'$  and  $B'$  from  $G_{A_1, A_2}^u(V, E)$  respectively. We define function  $RB(\pi)$  to represent “generalized” current running buffer size of a removal sequence  $\pi$ : When vertices in  $\pi$  are removed from the dependency graph, if the current running buffer size is positive, then  $RB(\pi)$  equals the number of running buffers; otherwise,  $RB(\pi)$  equals the negation of the number of empty goal poses. In the depth-first recursion, each node on the binary tree  $T$  is visited at most three times:

- 1) Before exploring child nodes. The peak may be reached during the removal of  $C'$ . Let  $\pi_{C^*}$  be the sequence when the running buffer size reaches the peak.  $RB(\pi_{C^*}) \leq RB(\pi_0) + 10\sqrt{2}\sqrt{|V|}$ .
- 2) After we deal with  $A'$  and before we deal with  $B'$ .  $RB(\pi_{A'}) = RB(\pi_0) + (s(C') - g(C')) + (s(A') - g(A'))$ .
- 3) After we deal with  $B'$ .  $RB(\pi_{B'}) = RB(\pi_0) + (s(V) - g(V))$ .

**Lemma IV.3.**  $RB(\pi_{A'}) \leq (RB(\pi_{C^*}) + RB(\pi_{B'}))/2$ .

*Proof.*

$$\begin{aligned}
& RB(\pi_{A'}) \\
&= RB(\pi_0) + (s(P) - g(P)) + (s(C') - g(C')) \\
&\quad + (s(A') - g(A')) \\
&= RB(\pi_0) + (s(P) - g(P)) + (s(C') - g(C')) \\
&\quad + \min[s(A') - g(A'), s(B') - g(B')] \\
&\leq RB(\pi_0) + (s(P) - g(P)) + (s(C') - g(C')) \\
&\quad + \frac{1}{2}[(s(V) - g(V)) - (s(P) - g(P)) \\
&\quad - (s(C') - g(C'))] \\
&= \frac{1}{2}\{[RB(\pi_0) + s(V) - g(V)] \\
&\quad + [RB(\pi_0) + (s(P) - g(P)) + (s(C') - g(C'))]\} \\
&= \frac{1}{2}[RB(\pi_{B'}) + RB(\pi_{C'})] \\
&\leq \frac{1}{2}[RB(\pi_{B'}) + RB(\pi_{C^*})]
\end{aligned}$$

□

Lemma IV.3 establishes the relationship among  $\pi_{C^*}$ ,  $\pi_{A'}$ , and  $\pi_{B'}$  of a node on  $T$ . With this lemma, we obtain an upper bound for each node:

**Lemma IV.4.** Given a node  $N$  with depth  $d$  in the binary tree  $T$ , let  $\pi_{C^*}(N)$ ,  $\pi_{A'}(N)$ , and  $\pi_{B'}(N)$  be  $\pi_{C^*}$ ,  $\pi_{A'}$ , and  $\pi_{B'}$  of  $N$  respectively.  $RB(\pi_{C^*}(N))$ ,  $RB(\pi_{A'}(N))$ , and  $RB(\pi_{B'}(N))$  are all upper bounded by

$$\frac{[1 - (\sqrt{\frac{2}{3}})^{d+1}]}{1 - \sqrt{\frac{2}{3}}} 20\sqrt{n} \quad (1)$$

where  $n$  is the number of objects in the instance.

*Proof.* The conclusion can be proven by induction.

When  $d = 0$ , the dependency graph at the root node  $r$  has  $n$  start vertices and  $n$  goal vertices. We have  $RB(\pi_{C^*}) \leq 20\sqrt{n}$ ,  $RB(\pi_{B'}) = 0$ . According to Lemma IV.3,  $RB(\pi_{A'}) \leq 10\sqrt{n}$ . The conclusion holds.

Assume that the conclusion holds for all the nodes with depth less than or equal to  $k$ . Given an arbitrary node  $N$  in the depth  $k$ , let the left and right children of  $N$  be  $L$  and  $R$ , which are the nodes with depth  $k + 1$ . The corresponding dependency graphs have at most  $(2/3)^{k+1} \cdot 2n$  vertices respectively.

$$RB(\pi_{C^*}(L)) \leq RB(\pi_{C^*}(N)) + \sqrt{(2/3)^{k+1} \cdot 2n} \cdot 10\sqrt{2}$$

$$RB(\pi_{C^*}(R)) \leq RB(\pi_{A'}(N)) + \sqrt{(2/3)^{k+1} \cdot 2n} \cdot 10\sqrt{2}$$

Since  $\pi_{B'}(L) = \pi_{A'}(N)$  and  $\pi_{B'}(R) = \pi_{B'}(N)$ , upper bound for nodes with depth  $k$  holds for  $\pi_{B'}(L)$  and  $\pi_{B'}(R)$ . Therefore, the running buffer size for the depth  $k + 1$  nodes

have an upper bound

$$\begin{aligned} & \frac{[1 - (\sqrt{2/3})^{k+1}]}{1 - \sqrt{2/3}} 20\sqrt{n} + \sqrt{(2/3)^{k+1} \cdot 2n \cdot 10\sqrt{2}} \\ &= \frac{[1 - (\sqrt{2/3})^{k+2}]}{1 - \sqrt{2/3}} 20\sqrt{n} \end{aligned} \quad (2)$$

Therefore, the upper bound holds for all the nodes of depth  $k + 1$ . With induction, the lemma holds.  $\square$

With Lemma IV.4, we have MRB is bounded by  $\frac{20}{1 - \sqrt{2/3}} \sqrt{n}$ .

**Theorem IV.2.** For URBM with  $n$  uniform cylinders, a polynomial time algorithm can compute a plan with  $O(\sqrt{n})$  RB, which implies that MRB is bounded by  $O(\sqrt{n})$ .

## V. FAST ALGORITHMS FOR LRBM AND URBM

In this section, we first describe a dynamic programming-based method for LRBM (Sec. V-A). Then, we propose a priority queue based method in Sec. V-B for URBM. Finally, a significantly faster depth-first modification of DP for computing MRB is provided in Sec. V-C. We mention that, we also developed an integer programming model, denoted  $TB_{MRB}$ , for computing the minimum total number of buffers needed subject to the MRB constraint, which is compared with the algorithm that computes the minimum total buffer without the MRB constraint, denoted as  $TB_{FVS}$ , from [1]. A brief description of  $TB_{MRB}$  is given in Sec. V-D.

### A. Dynamic Programming (DP) for LRBM

As mentioned in Sec. III-B, a rearrangement plan in LRBM can be represented as a linear ordering of object labels where objects will be moved out of the start pose based on the order. That is, given an ordering of objects,  $\pi$ , we start with  $o_{\pi(1)}$ . If  $x_{\pi(1)}^g$  is not occupied, then  $o_{\pi(1)}$  is directly moved there. Otherwise, it is moved to buffer location. We then continue with the second object in the order, and so on. After we work with each object in the given order, we always check whether objects in buffer can be moved to their goals, and do so if an opportunity presents. We now describe a *dynamic programming* (DP) algorithm for computing an ordering that yields the MRB.

The pseudo-code of the algorithm is given in Algo. 2. The algorithm maintains a search tree  $T$ , each node of which represents an arrangement where a set of objects  $S$  have left the corresponding start poses. We record the objects currently at the buffer ( $T[S].b$ ) and the minimum running buffer from the start arrangement  $\mathcal{A}_1$  to the current arrangement ( $T[S].MRB$ ). The DP starts with an empty  $T$ . We let the root node represent  $\mathcal{A}_1$  (line 1). At this moment, there is no object in the buffer and the MRB is 0 (line 2-3). And then we enumerate all the arrangements with  $|S| = 1, 2, \dots$  and finally  $n$  (line 4-5). For arbitrary  $S$ , the objects at the buffer are the objects in  $S$  whose goal poses are still occupied by other objects (line 6), i.e.,  $\{o \in S \mid \exists o' \in \mathcal{O} \setminus S, (o, o') \in A\}$ , where  $A$  is the set of arcs in  $G_{\mathcal{A}_1, \mathcal{A}_2}^\ell$ .  $T[S].MRB$ , the minimum running buffer from the root node  $T[\emptyset]$  to  $T[S]$ ,

depends on the last object  $o_i$  added into  $S$  and can be computed by enumerating  $o_i$  (line 7-20):

$$T[S].MRB = \min_{o_i \in S} \max(T[S \setminus \{o_i\}].MRB, |T[S].b|, |T[S \setminus \{o_i\}].b| + TC(S \setminus \{o_i\}, S)),$$

where the *transition cost*  $TC$  is given as

$$TC(S \setminus \{o_i\}, S) = \begin{cases} 1, & o_i \in T[S].b, \\ 0, & \text{otherwise,} \end{cases}$$

with  $x_i^g$  currently occupied (line 10), the transition cost is due to objects dependent on  $o_i$  cannot be moved out of the buffer before moving  $o_i$  to the buffer (line 11). If  $T[S].MRB$  is minimized with  $o_i$  being the last object in  $S$  from the starts, then  $T[S \setminus \{o_i\}]$  is the parent node of  $T[S]$  in  $T$  (line 14-16). Once  $T[\mathcal{O}]$  is added into  $T$ ,  $T[\mathcal{O}].MRB$  is the MRB of the instance (line 17) and the path in  $T$  from  $T[\emptyset]$  to  $T[\mathcal{O}]$  is the corresponding solution to the instance.

### Algorithm 2: Dynamic Programming

---

**Input :**  $G_{\mathcal{A}_1, \mathcal{A}_2}(\mathcal{O}, A)$ : labeled dependency graph  
**Output:** MRB: the minimum number of running buffers

```

1  $T.root \leftarrow \emptyset$ 
2  $T[\emptyset].b \leftarrow \emptyset$  % objects currently at the buffer
3  $T[\emptyset].MRB \leftarrow 0$  % current minimum running buffer
4 for  $1 \leq k \leq |\mathcal{O}|$  do
    % enumerate cases where  $k$  objects have
    % left the start poses
5   for  $S \in k\text{-combinations of } \mathcal{O}$  do
6      $T[S].b \leftarrow \{o \in S \mid \exists o' \in \mathcal{O} \setminus S, (o, o') \in A\}$ 
7     % Find the MRB from  $T[\emptyset]$  to  $T[S]$ 
8      $T[S].MRB \leftarrow \infty$ 
9     for  $o_i \in S$  do
10       $parent = S \setminus \{o_i\}$ 
11      if  $o_i \in T[S].b$  then
12         $RB \leftarrow \max(T[parent].MRB, |T[S].b|,$ 
13           $|T[parent].b| + 1)$ 
14      else
15         $RB \leftarrow \max(T[parent].MRB, |T[S].b|)$ 
16      if  $RB < T[S].MRB$  then
17         $T[S].MRB \leftarrow RB$ 
18         $T[S].parent \leftarrow parent$ 
19 return  $T[\mathcal{O}].MRB$ 
```

---

For the LRBM instance in Fig. 2, Tab. I shows  $T[S].MRB$  with different last-object options when  $S = \{o_2, o_5, o_6\}$ . If the last object  $o_i$  is  $o_5$ , then we need to move  $o_5$  into the buffer before moving  $o_6$  out of the buffer. Therefore, even though buffer sizes of the parent node and the current node are both 2, there is a moment when all of the three objects are at the buffer. However, when we choose  $o_2$  or  $o_6$  as the last object to add, the  $T[S].MRB$  becomes 2.

TABLE I.  $T[S].MRB$  for different last objects ( $[p] = [parent]$ )

Last object	$T[p].MRB$	$T[p].b$	$T[S].b$	$T[S].MRB$
$o_2$	1	$\{o_5\}$	$\{o_2, o_5\}$	2
$o_5$	2	$\{o_2, o_6\}$	$\{o_2, o_5\}$	3
$o_6$	2	$\{o_2, o_5\}$	$\{o_2, o_5\}$	2

### B. A Priority Queue based method for URBM

Similar to LRBM, rearrangement plans in URBM can be represented by a linear ordering of goal vertices in  $G_{\mathcal{A}_1, \mathcal{A}_2}^u$ .



We can compute the ordering that yields MRB by maintaining a search tree like in Algo. 2. Each node  $T[V]$  in the tree represents an arrangement where a set of goal vertices  $V$  have been filled. The remaining dependencies of  $T[V]$  is an induced graph of  $G_{\mathcal{A}_1, \mathcal{A}_2}^u$ , formed from  $V(G_{\mathcal{A}_1, \mathcal{A}_2}^u) \setminus (V \cup N(V))$  where  $N(V)$  is the neighbors of  $V$  in  $G_{\mathcal{A}_1, \mathcal{A}_2}^u$ . The running buffer size of  $T[V]$  is  $|N(V)| - |V|$ . Given an induced graph  $I(V)$ , denote the goal vertices with no more than one neighbor in  $I(V)$  as *free goals*. We make two observations. First, given an induced graph  $I(V)$ , we can always prioritize the free goals in terms of the order to fill without optimality loss. Second, multiple free goals may be generated as a goal vertex is filled. For example, in the instance shown in Fig. 2(a), when the goal representing  $c_g^5$  is filled,  $c_g^2$ ,  $c_g^3$ , and  $c_g^4$  become free goals and can be added to the linear ordering in an arbitrary order. In conclusion, the necessary nodes (nodes without free goals in the induced graph) in the search tree are sparse and enumerating nodes with DP carries much overhead.

As such, instead of exploring the search tree layer by layer like DP, we maintain a sparse tree with a priority queue  $Q$ . While each node still represents an arrangement, each edge in the tree represents either an action moving an object to the buffer or multiple actions filling free goal poses. We always pop out and develop the node with the smallest MRB in  $Q$ . If a child node of the one that we develop already exist in the tree but is with smaller MRB than previously claimed, we will update the parent of the child node into the node we are developing. The MRB of the node representing  $\mathcal{A}_2$  sets an upper bound of the solution and nodes in  $Q$  with larger MRB will be pruned away. The algorithm terminates when  $Q$  is empty. We denote this priority queue-based search method PQS.

### C. Dynamic Programming with Depth-First Exploration

Both LRBM and URBM can be viewed as solving a series of decision problems, i.e., asking whether we can find a rearrangement plan with  $k = 1, 2, \dots$  running buffers. As dynamic programming is applied to solve such decision problems, instead of performing the more standard breadth first exploration of the search tree, we identified that a depth-first exploration is much more effective. We call this variation of dynamic programming, which is a fairly straightforward alteration of a standard DP procedure. Essentially, DFDP fixes a  $k$  and checks whether there is a plan requiring no more than  $k$  running buffers. As the search tree (see Sec. V-A) is explored, depth-first exploration is used instead of breadth-first. The intuition is that, when there are many rearrangement plans on the search tree that do not use more than  $k$  running buffers, depth-first search will quickly find such a solution, whereas a standard DP must grow the full search tree before returning a feasible solution. A similar depth-first exploration heuristic is used in [58].

### D. Minimizing Total Buffers Subject to MRB Constraints

Let binary variables  $c_{i,j}$  represent  $G_{\mathcal{A}_1, \mathcal{A}_2}^{\ell}$ :  $c_{i,j} = 1$  if and only if  $(i, j)$  is in the arc set of  $G_{\mathcal{A}_1, \mathcal{A}_2}^{\ell}$ . Let  $y_{i,j}$  ( $1 \leq i < j \leq$

$n$ ) be the binary sequential variables:  $y_{i,j} = 1$  if and only if  $o_i$  moves out of the start pose before  $o_j$ . We further introduce two sets of binary variables  $g_{i,j}$  and  $b_{i,j}$  ( $1 \leq i, j \leq n$ ) to indicate object positions at each moment.  $g_{i,j} = 1$  indicates that  $o_j$  has no dependency on other objects when moving  $o_i$  from the start pose. In other words, the goal pose of  $o_j$  is available at the moment.  $b_{i,j} = 1$  indicates that  $o_j$  stays at the buffer after moving  $o_i$  away from the start pose. Finally, binary variables  $B_i = 1$  if and only if  $o_i$  is moved to a buffer at some point. The objective function consists of two terms: the total buffer term and running buffer term. The total buffer term, scaled by  $\alpha$ , counts the number of objects that need buffer locations. The running buffer is represented with an integer variable  $K$  and scaled by  $\beta$ . To minimize total buffers subject to MRB constraints, we set  $\alpha = 1, \beta = n$ . The objective function is adaptive for different demands on rearrangement plans. Specifically, when  $\alpha = 0, \beta > 0$ , the MIP model minimizes MRB. When  $\alpha > 0, \beta = 0$ , the MIP model minimizes total buffers, i.e. total actions in the rearrangement plan. When  $\alpha/\beta > n - 1$ , the MIP model first minimizes total buffers, and then minimizes running buffers.

In the MIP model, Constraints 4 imply the rules for sequential variables. Constraints 5 imply that  $B_j = 1$  if  $o_j$  has been at buffers in the plan. Constraints 6 imply that the running buffer  $K$  is lower bounded by the maximum number of objects concurrently placed in buffers. With Constraints 7 and 8,  $g_{i,j} = 0$  if and only if  $o_j$  depends on an object  $o_k$  which is still at the start pose when  $o_i$  is moved. With Constraints 9-11,  $b_{i,j} = 1$  if and only if  $o_j$  is moved before  $o_i$  and the goal pose is still unavailable when  $o_i$  is moved from the start pose.

$$\arg \min \alpha \left[ \sum_{i=1}^n B_i \right] + \beta K \quad (3)$$

$$0 \leq y_{i,j} + y_{j,k} - y_{i,k} \leq 1 \quad \forall 1 \leq i < j < k \leq n \quad (4)$$

$$B_j \geq \sum_{1 \leq i \leq n} \frac{b_{i,j}}{n} \quad \forall 1 \leq j \leq n \quad (5)$$

$$K \geq \sum_{1 \leq j \leq n} b_{i,j} \quad \forall 1 \leq i \leq n \quad (6)$$

$$\sum_{1 \leq k < i} \frac{c_{j,k}(1 - y_{k,i})}{n} + \sum_{i < k \leq n} \frac{c_{j,k}y_{i,k}}{n} \leq 1 - g_{i,j} \quad (7)$$

$$1 - g_{i,j} \leq \sum_{1 \leq k < i} c_{j,k}(1 - y_{k,i}) + \sum_{i < k \leq n} c_{j,k}y_{i,k} \quad (8)$$

$$\frac{g_{i,j} + y_{i,j}}{2} \leq 1 - b_{i,j} \leq g_{i,j} + y_{i,j} \quad (9)$$

$$\frac{g_{j,i} + (1 - y_{i,j})}{2} \leq 1 - b_{j,i} \leq g_{j,i} + (1 - y_{i,j}) \quad (10)$$

$$b_{i,i} = 1 - g_{i,i} \quad (11)$$

## VI. EXPERIMENTAL STUDIES

Our evaluation focuses on uniform cylinders, given their prevalence in practical applications. For simulation studies, instances with different object densities are created, as measured by *density level*  $\rho := n\pi r^2/(h * w)$ , where  $n$  is the number of objects and  $r$  is the base radius.  $h$  and  $w$  are the height and width of the workspace. In other words,  $\rho$  is the proportion of the tabletop surface occupied by objects.

The evaluation is conducted on both random object placements and manually constructed difficult setups (e.g., dependency grids with  $MRB = \Omega(\sqrt{n})$ ). For generating test cases with high  $\rho$  value, we invented a physic engine (we used Gazebo) based approach for doing so. Within a rectangular box, we sample placements of cylinders at lower density and then also sample locations for some smaller “filler” objects (see Fig. 11, left). From here, one side of the box is pushed to reach a high density setting (Fig. 11, right), which is very difficult to generate via random sampling. By controlling the ratio of the two types of objects, different density levels can be readily obtained. Fig. 12 shows three random object placements for  $\rho = 0.2, 0.4$  and  $0.6$ .

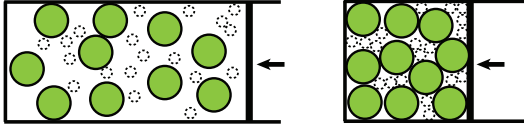


Fig. 11: Generating dense instances using a physics-engine based simulator through compression of the left scene to the right scene.

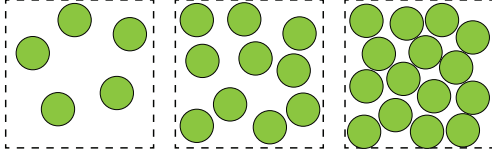


Fig. 12: Unlabeled arrangements with  $\rho = 0.2, 0.4, 0.6$  respectively.

From two randomly generated object placements with same  $\rho$  and  $n$  values, a URBM instance can be readily created by superimposing one over the other. LRBM instances can be generated from URBM instances by assigning each object a random label in  $[n]$  for both start and goal configurations.

The proposed algorithms are implemented in Python and all experiments are executed on an Intel® Xeon® CPU at 3.00GHz. For solving ILP, Gurobi 9.16.0 [59] is used.

### A. Labeled Rearrangement over Random Instances

In Fig. 13, we compare the effectiveness of the DP and DFDP, in terms of computation time and success rate, for different densities. Each data point is the average of 30 test cases minus the unfinished ones, if any, subject to a time limit of 300 seconds per test case. For LRBM, we are able to push to  $\rho = 0.4$ , which is fairly dense. The results clearly demonstrate that DFDP significantly outperform the baseline DP. Based on the evaluation, both methods can be used to tackle practical sized problems (e.g., tens of objects), with DFDP demonstrating superior efficiency and robustness.

The actual MRB sizes for the same test cases from Fig. 13 are shown in Fig. 14 on the left. We observe that MRB is rarely very large even for fairly large LRBM instances. The

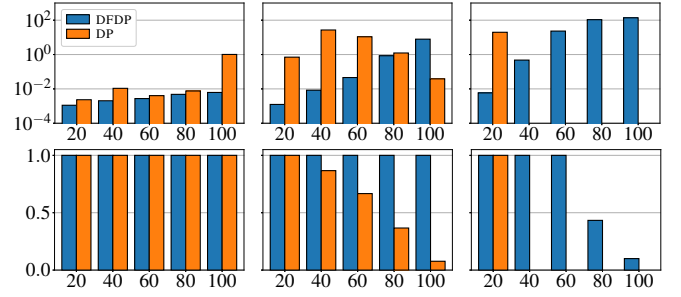


Fig. 13: Performance of DFDP and DP over LRBM. The top row shows the average computation time (s) and the bottom row the success rate, for density levels  $\rho = 0.2, 0.3, 0.4$ , from left to right. The  $x$ -axis denotes the number of objects involved in a test case.

size of MRB appears correlated to the size of the largest connected component of the underlying dependency graph, shown in Fig. 14 on the right.

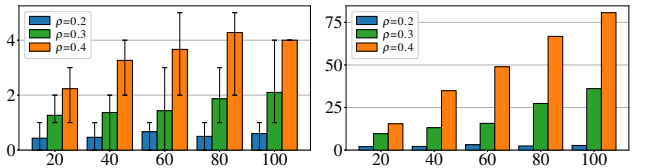


Fig. 14: For LRBM instances with  $\rho = 0.2-0.4$  and  $n = 20-100$ , the left figure shows average MRB size and range. The right figure shows the size of the largest connected component of the dependency graph.

For LRBM with  $\rho = 0.3$  and  $n$  up to 50, we computed the MFVS sizes using  $TB_{FVS}$  (which does not scale to higher  $\rho$  and  $n$ ) and compared that with the MRB sizes, as shown in Fig. 15 (a). We observe that the MFVS is about twice as large as MRB, suggesting that MRB provides more reliable information for estimating the design parameters of pick-n-place systems. For these instances, we also computed the total number of buffers needed subject to the MRB constraint using  $TB_{MRB}$ . Out of about 150 instances, only 1 showed a difference as compared with MFVS (therefore, this information is not shown in the figure). In Fig. 15 (b), we provided computation time comparison between  $TB_{FVS}$  and  $TB_{MRB}$ , showing that  $TB_{MRB}$  is practical, if it is desirable to minimize the total buffers after guaranteeing the minimum number of running buffers.

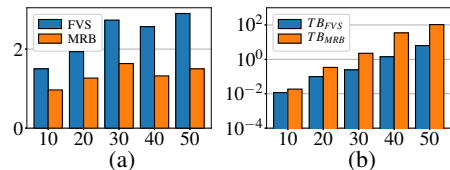


Fig. 15: (a) Comparison between size of MRB and MFVS. (b) Computation time comparison between  $TB_{FVS}$  and  $TB_{MRB}$ .

Considering our theoretical findings and the evaluation results, an important conclusion can be drawn here is that MRB is effectively a small constant for random instances, even when the instances are very large. Also, minimizing the total number of buffers used subject to MRB constraint can be done quickly for practical sized problems.

### B. Unlabeled Rearrangement over Random Instances

For URBM, we carry out similar performance evaluation as we have done for LRBM. Here, PQS and DFDP are compared. For each combination of  $\rho$  and  $n$ , 100 random test cases are evaluated. Notably, we can reach  $\rho = 0.6$  with relative ease. From Fig. 16, we observe that DFDP is more efficient than PQS, especially for large-scale dense settings. In terms of the MRB size, all instances tested has an average MRB size between 0 and 0.7, which is fairly small (Fig. 17). Interestingly, we witness a decrease of MRB as the number of objects increases, which could be due to the lessening “border effect” of the larger instances. That is, for instances with fewer objects, the bounding square puts more restriction on the placement of the objects inside. For larger instances, such restricting effects become smaller. We mention that the total number of buffers for random URBM cases subject to MRB constraints are generally very small.

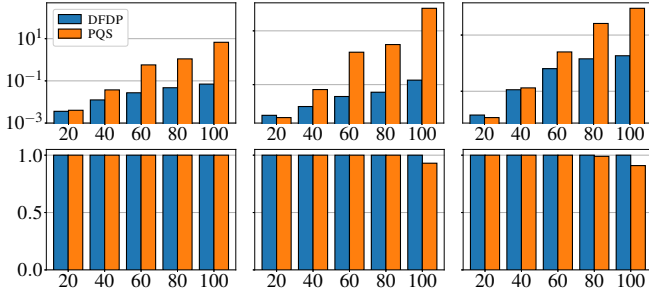


Fig. 16: Performance of DFDP and PQS over URBM. The top row shows the average computation time and the bottom row shows the success rate, for density levels  $\rho = 0.4, 0.5, 0.6$ , from left to right.

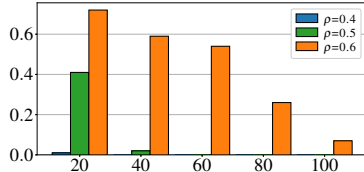


Fig. 17: Average MRB size for URBM instances with  $\rho = 0.4 - 0.6$  and  $n = 20 - 100$ . For  $\rho = 0.4$  and  $0.5$ , the MRB sizes are near zero as the number of objects goes beyond 20.

### C. Manually Constructed Difficult Cases

In the random scenario, the running buffer size is limited. In particular, for LRBM, the dependency graph tends to consist of multiple strongly connected components that can be dealt with independently. We further show the performance of DFDP on the instances with  $\text{MRB} = \Theta(\sqrt{n})$ . We evaluate three kinds of instances: (1) UG:  $m^2$ -object URBM instances whose  $G_{A_1, A_2}^u$  are dependency grid  $\mathcal{D}(m, 2m)$  (e.g., Fig. 7); (2) LG:  $m^2$ -object LRBM instances whose start and goal arrangements are the same as the instances in (1). (3) LC:  $m^2$ -object LRBM instances with objects placed on a cycle (Fig. 9). The computation time and the corresponding MRB are shown in Fig. 18. For LG instances, the labels are randomly assigned. We try 30 test cases and then plot out the average. We observe that the MRB are much larger for these handcrafted instances as compared with random instances with similar density and number of objects.

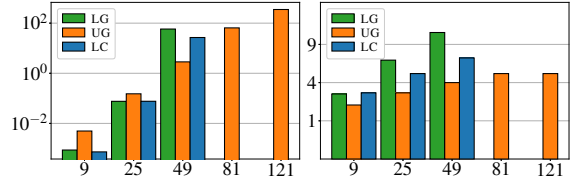


Fig. 18: For handcrafted cases and different number of objects, the left figure shows the computation time by DFDP and the right figure the resulting MRB size.

## VII. CONCLUSION AND DISCUSSION

In this work, we investigate the problem of minimizing the number of running buffers (MRB) for solving labeled and unlabeled tabletop rearrangement problems with overhand grasps (TORO), which translates to finding a best linear ordering of vertices of the associated underlying dependency graph. For TORO, MRB is an important quantity to understand as it determines the problem’s feasibility if only external buffers are to be used, which is the case in some real-world applications [1]. Despite the provably high computational complexity that is involved, we provide effective dynamic programming-based algorithms capable of quickly computing MRB for large and dense labeled/unlabeled TORO instances. In addition, we also provide methods for minimizing the total number of buffers subject to MRB constraints. Whereas we prove that MRB can grow unbounded for both labeled and unlabeled settings for special cases for uniform cylinders, empirical evaluations suggest that real-world random TORO instances are likely to have much smaller MRB values.

We conclude by leaving the readers with some interesting open problems. On the structural side, while LRBM in general is proven to be NP-Hard, the computational intractability of either LRBM with uniform cylinders or URBM in general remains unresolved. As for bounds, the lower and upper bounds of MRB for LRBM for uniform cylinders do not yet agree; can the bound gap be narrowed further?

## REFERENCES

- [1] S. D. Han, N. M. Stiffler, A. Krontiris, K. E. Bekris, and J. Yu, “Complexity results and fast methods for optimal tabletop rearrangement with overhand grasps,” *The International Journal of Robotics Research*, vol. 37, no. 13-14, pp. 1775–1795, 2018.
- [2] A. Saxena, J. Driemeyer, and A. Y. Ng, “Robotic grasping of novel objects using vision,” *The International Journal of Robotics Research*, vol. 27, no. 2, pp. 157–173, 2008.
- [3] M. Gualtieri, A. Ten Pas, K. Saenko, and R. Platt, “High precision grasp pose detection in dense clutter,” in *2016 IEEE/RSJ International Conference on Intelligent Robots and Systems (IROS)*. IEEE, 2016, pp. 598–605.
- [4] C. Mitash, K. E. Bekris, and A. Boularias, “A self-supervised learning system for object detection using physics simulation and multi-view pose estimation,” in *2017 IEEE/RSJ International Conference on Intelligent Robots and Systems (IROS)*. IEEE, 2017, pp. 545–551.
- [5] Y. Xiang, T. Schmidt, V. Narayanan, and D. Fox, “Posecnn: A convolutional neural network for 6d object pose estimation in cluttered scenes,” in *Robotics: Science and Systems*, 2018.
- [6] O. Ben-Shahar and E. Rivlin, “Practical pushing planning for rearrangement tasks,” *IEEE Transactions on Robotics and Automation*, vol. 14, no. 4, pp. 549–565, 1998.
- [7] M. Stilman and J. J. Kuffner, “Navigation among movable obstacles: Real-time reasoning in complex environments,” *International Journal of Humanoid Robotics*, vol. 2, no. 04, pp. 479–503, 2005.

- [8] K. Treleaven, M. Pavone, and E. Frazzoli, "Asymptotically optimal algorithms for one-to-one pickup and delivery problems with applications to transportation systems," *IEEE Transactions on Automatic Control*, vol. 58, no. 9, pp. 2261–2276, 2013.
- [9] G. Havur, G. Ozbilgin, E. Erdem, and V. Patoglu, "Geometric rearrangement of multiple movable objects on cluttered surfaces: A hybrid reasoning approach," in *2014 IEEE International Conference on Robotics and Automation (ICRA)*. IEEE, 2014, pp. 445–452.
- [10] J. A. Haustein, J. King, S. S. Srinivasa, and T. Asfour, "Kinodynamic randomized rearrangement planning via dynamic transitions between statically stable states," in *2015 IEEE International Conference on Robotics and Automation (ICRA)*. IEEE, 2015, pp. 3075–3082.
- [11] A. Krontiris and K. E. Bekris, "Dealing with difficult instances of object rearrangement," in *Robotics: Science and Systems*, vol. 1123, 2015.
- [12] J. E. King, M. Cagnetti, and S. S. Srinivasa, "Rearrangement planning using object-centric and robot-centric action spaces," in *2016 IEEE International Conference on Robotics and Automation (ICRA)*. IEEE, 2016, pp. 3940–3947.
- [13] E. Huang, Z. Jia, and M. T. Mason, "Large-scale multi-object rearrangement," in *2019 International Conference on Robotics and Automation (ICRA)*. IEEE, 2019, pp. 211–218.
- [14] J. Lee, Y. Cho, C. Nam, J. Park, and C. Kim, "Efficient obstacle rearrangement for object manipulation tasks in cluttered environments," in *2019 International Conference on Robotics and Automation (ICRA)*. IEEE, 2019, pp. 183–189.
- [15] Z. Pan and K. Hauser, "Decision making in joint push-grasp action space for large-scale object sorting," *arXiv preprint arXiv:2010.10064*, 2020.
- [16] R. H. Taylor, M. T. Mason, and K. Y. Goldberg, "Sensor-based manipulation planning as a game with nature," in *Fourth International Symposium on Robotics Research*, 1987, pp. 421–429.
- [17] K. Y. Goldberg, "Orienting polygonal parts without sensors," *Algorithmica*, vol. 10, no. 2, pp. 201–225, 1993.
- [18] K. M. Lynch and M. T. Mason, "Dynamic nonprehensile manipulation: Controllability, planning, and experiments," *The International Journal of Robotics Research*, vol. 18, no. 1, pp. 64–92, 1999.
- [19] M. Dogar and S. Srinivasa, "A framework for push-grasping in clutter," *Robotics: Science and systems VII*, vol. 1, 2011.
- [20] J. Bohg, A. Morales, T. Asfour, and D. Kragic, "Data-driven grasp synthesis—a survey," *IEEE Transactions on Robotics*, vol. 30, no. 2, pp. 289–309, 2013.
- [21] N. C. Daffe, A. Rodriguez, R. Paolini, B. Tang, S. S. Srinivasa, M. Erdmann, M. T. Mason, I. Lundberg, H. Staab, and T. Fuhlbrigge, "Extrinsic dexterity: In-hand manipulation with external forces," in *2014 IEEE International Conference on Robotics and Automation (ICRA)*. IEEE, 2014, pp. 1578–1585.
- [22] A. Boularias, J. Bagnell, and A. Stentz, "Learning to manipulate unknown objects in clutter by reinforcement," in *Proceedings of the AAAI Conference on Artificial Intelligence*, vol. 29, no. 1, 2015.
- [23] N. Chavan-Daffe and A. Rodriguez, "Prehensile pushing: In-hand manipulation with push-primitives," in *2015 IEEE/RSJ International Conference on Intelligent Robots and Systems (IROS)*. IEEE, 2015, pp. 6215–6222.
- [24] L. P. Kaelbling and T. Lozano-Pérez, "Hierarchical task and motion planning in the now," in *2011 IEEE International Conference on Robotics and Automation*. IEEE, 2011, pp. 1470–1477.
- [25] S. Levine, C. Finn, T. Darrell, and P. Abbeel, "End-to-end training of deep visuomotor policies," *The Journal of Machine Learning Research*, vol. 17, no. 1, pp. 1334–1373, 2016.
- [26] J. Mahler, J. Liang, S. Niyaz, M. Laskey, R. Doan, X. Liu, J. A. Ojea, and K. Goldberg, "Dex-net 2.0: Deep learning to plan robust grasps with synthetic point clouds and analytic grasp metrics," *arXiv preprint arXiv:1703.09312*, 2017.
- [27] A. Zeng, S. Song, K.-T. Yu, E. Donlon, F. R. Hogan, M. Bauza, D. Ma, O. Taylor, M. Liu, E. Romo, *et al.*, "Robotic pick-and-place of novel objects in clutter with multi-affordance grasping and cross-domain image matching," in *2018 IEEE international conference on robotics and automation (ICRA)*. IEEE, 2018, pp. 3750–3757.
- [28] A. M. Wells, N. T. Dantam, A. Shrivastava, and L. E. Kavvaki, "Learning feasibility for task and motion planning in tabletop environments," *IEEE robotics and automation letters*, vol. 4, no. 2, pp. 1255–1262, 2019.
- [29] J. E. Hopcroft, J. T. Schwartz, and M. Sharir, "On the complexity of motion planning for multiple independent objects; pspace-hardness of the 'warehouseman's problem'," *The International Journal of Robotics Research*, vol. 3, no. 4, pp. 76–88, 1984.
- [30] G. Wilfong, "Motion planning in the presence of movable obstacles," *Annals of Mathematics and Artificial Intelligence*, vol. 3, no. 1, pp. 131–150, 1991.
- [31] M. Stilman, J.-U. Schamburek, J. Kuffner, and T. Asfour, "Manipulation planning among movable obstacles," in *Proceedings 2007 IEEE international conference on robotics and automation*. IEEE, 2007, pp. 3327–3332.
- [32] C. H. Papadimitriou, "The euclidean travelling salesman problem is np-complete," *Theoretical computer science*, vol. 4, no. 3, pp. 237–244, 1977.
- [33] R. M. Karp, "Reducibility among combinatorial problems," in *Complexity of computer computations*. Springer, 1972, pp. 85–103.
- [34] S. Bereg and A. Dumitrescu, "The lifting model for reconfiguration," *Discrete & Computational Geometry*, vol. 35, no. 4, pp. 653–669, 2006.
- [35] C. Nam, J. Lee, Y. Cho, J. Lee, D. H. Kim, and C. Kim, "Planning for target retrieval using a robotic manipulator in cluttered and occluded environments," *arXiv preprint arXiv:1907.03956*, 2019.
- [36] D. Halperin, M. van Kreveld, G. Miglioli-Levy, and M. Sharir, "Space-aware reconfiguration," *arXiv preprint arXiv:2006.04402*, 2020.
- [37] L. Chang, J. R. Smith, and D. Fox, "Interactive singulation of objects from a pile," in *2012 IEEE International Conference on Robotics and Automation*. IEEE, 2012, pp. 3875–3882.
- [38] M. Laskey, J. Lee, C. Chuck, D. Gealy, W. Hsieh, F. T. Pokorny, A. D. Dragan, and K. Goldberg, "Robot grasping in clutter: Using a hierarchy of supervisors for learning from demonstrations," in *2016 IEEE International Conference on Automation Science and Engineering (CASE)*. IEEE, 2016, pp. 827–834.
- [39] A. Eitel, N. Hauß, and W. Burgard, "Learning to singulate objects using a push proposal network," in *Robotics research*. Springer, 2020, pp. 405–419.
- [40] H. Song, J. A. Haustein, W. Yuan, K. Hang, M. Y. Wang, D. Kragic, and J. A. Stork, "Multi-object rearrangement with monte carlo tree search: A case study on planar nonprehensile sorting," *arXiv:1912.07024*, 2019.
- [41] J. van Den Berg, J. Snoeyink, M. C. Lin, and D. Manocha, "Centralized path planning for multiple robots: Optimal decoupling into sequential plans," in *Robotics: Science and systems*, vol. 2, no. 2.5, 2009, pp. 2–3.
- [42] J. Díaz, J. Petit, and M. Serna, "A survey of graph layout problems," *ACM Computing Surveys (CSUR)*, vol. 34, no. 3, pp. 313–356, 2002.
- [43] M. R. Garey and D. S. Johnson, "Vertex ordering," in *Computers and Intractability: a Guide to The Theory of NP-Completeness*, 1979, pp. 199–201.
- [44] C. H. Papadimitriou, "The np-completeness of the bandwidth minimization problem," *Computing*, vol. 16, no. 3, pp. 263–270, 1976.
- [45] M. R. Garey, D. S. Johnson, and L. Stockmeyer, "Some simplified np-complete problems," in *Proceedings of the sixth annual ACM symposium on Theory of computing*, 1974, pp. 47–63.
- [46] F. Gavril, "Some np-complete problems on graphs," John Hopkins University, Baltimore, MD, 1977, pp. 91–95.
- [47] H. L. Bodlaender, J. R. Gilbert, H. Hafsteinsson, and T. Kloks, "Approximating treewidth, pathwidth, frontsize, and shortest elimination tree," *Journal of Algorithms*, vol. 18, no. 2, pp. 238–255, 1995.
- [48] T.-h. Shin, H. Oh, and S. Ha, "Minimizing buffer requirements for throughput constrained parallel execution of synchronous dataflow graph," in *16th Asia and South Pacific Design Automation Conference (ASP-DAC 2011)*. IEEE, 2011, pp. 165–170.
- [49] R. J. Lipton and R. E. Tarjan, "A separator theorem for planar graphs," *SIAM Journal on Applied Mathematics*, vol. 36, no. 2, pp. 177–189, 1979.
- [50] J. R. Gilbert, J. P. Hutchinson, and R. E. Tarjan, "A separator theorem for graphs of bounded genus," *Journal of Algorithms*, vol. 5, no. 3, pp. 391–407, 1984.
- [51] N. Alon, P. Seymour, and R. Thomas, "A separator theorem for graphs with an excluded minor and its applications," in *Proceedings of the twenty-second annual ACM symposium on Theory of computing*, 1990, pp. 293–299.
- [52] U. Elsner, *Graph partitioning-a survey*. Techn. Univ., 1997.
- [53] Y. Shiloach, "A minimum linear arrangement algorithm for undirected trees," *SIAM Journal on Computing*, vol. 8, no. 1, pp. 15–32, 1979.
- [54] D. Adolphson and T. C. Hu, "Optimal linear ordering," *SIAM Journal on Applied Mathematics*, vol. 25, no. 3, pp. 403–423, 1973.



- [55] L. M. Kirousis and C. H. Papadimitriou, "Searching and pebbling," *Theoretical Computer Science*, vol. 47, pp. 205–218, 1986.
- [56] N. G. Kinnarsley, "The vertex separation number of a graph equals its path-width," *Information Processing Letters*, vol. 42, no. 6, pp. 345–350, 1992.
- [57] M. R. Fellows and M. A. Langston, "On search decision and the efficiency of polynomial-time algorithms," in *Proceedings of the twenty-first annual ACM symposium on Theory of computing*, 1989, pp. 501–512.
- [58] R. Wang, K. Gao, D. Nakhimovich, J. Yu, and K. E. Bekris, "Uniform object rearrangement: From complete monotone primitives to efficient non-monotone informed search," *arXiv preprint arXiv:2101.12241*, 2021.
- [59] L. Gurobi Optimization, "Gurobi optimizer reference manual," 2021. [Online]. Available: <http://www.gurobi.com>